

Electronic Raman Scattering in High- T_c Superconductors: A Probe of $d_{x^2-y^2}$ Pairing

T. P. Devereaux,^{1,*} D. Einzel,² B. Stadlober,² R. Hackl,² D. H. Leach,¹ and J. J. Neumeier^{2,†}

¹Max-Planck-Institut für Festkörperforschung, Heisenbergstrasse 1, D-70569 Stuttgart, Federal Republic of Germany

²Walther-Meißner-Institut für Tieftemperaturforschung, D-85748 Garching, Federal Republic of Germany

(Received 23 July 1993)

New measurements on the high-temperature superconductor $\text{Bi}_2\text{Sr}_2\text{CaCu}_2\text{O}_8$ are interpreted and found to be in quantitative agreement with a theory for electronic Raman scattering in superconductors with $d_{x^2-y^2}$ pairing symmetry. The theory explains in a natural way, why the shape of the scattering intensity, as well as its change with temperature can be polarization (symmetry) dependent and hence resolves a controversy in previous interpretations of data on the electronic Raman effect.

PACS numbers: 74.25.Gz, 74.72.Hs, 78.30.Er

The nature of the pair state is one of the keys to solve the puzzle of superconductivity in the copper oxides. The repulsive Coulomb interaction which in part leads to the strong electronic correlations would indicate that these systems prefer not to condense into an s -wave superconducting state at low temperatures. Therefore order parameters with a node structure such as the pair state with $d_{x^2-y^2}$ symmetry have been considered alternatively as possible candidates for high- T_c superconductors [1]. Evidence for this type of gap comes in part from experiments which test the theoretically predicted low-temperature power laws for various thermodynamic and transport properties. These experiments measure only averages over the Fermi surface [2]. A method that uniquely probes the ground state symmetry, however, must allow for testing the gap at different parts of the Fermi surface. An example of such a method is electronic Raman scattering due to the breaking of Cooper pairs. It is well known that Raman scattering enables one to measure various symmetry degrees of freedom by simply rotating the incident and scattered photon polarization orientations. As a consequence, the Raman results provide a wealth of polarization-dependent information that turns out to be useful for determining the actual gap symmetry [3]. The existing body of data on the cuprate systems reveal four main points: (i) in contrast to conventional superconductors such as Nb_3Sn , no clear well-defined gap is seen for any polarization orientation even at the lowest temperatures measured [4], (ii) the peak of the low temperature electronic spectrum lies roughly at 30% higher frequency shifts for the polarization orientation which selects the (x^2-y^2) symmetry compared to all other symmetries [5,6], (iii) the low frequency Raman intensities vary roughly as ω^3 for the (x^2-y^2) symmetry and linearly in ω for the others [7], and (iv) the ratio of the residual scattering in the superconducting state to the normal state is smallest for the (x^2-y^2) case compared to all other configurations [7]. Such a rich spectrum of information should provide a stringent test of various candidates for pairing states.

The purpose of the present paper is to investigate the polarization dependence of the Raman spectra of a superconductor with $d_{x^2-y^2}$ symmetry. We calculate the gauge invariant electronic Raman scattering for a tetrag-

onal superconductor at finite temperatures and for various polarization orientations and give a quantitative comparison with Raman measurements on recently synthesized single crystals of the double-layer Bi system ($\text{Bi}_2:2:1:2$).

For this comparison we used single crystals of (i) as grown $\text{Bi}_2\text{Sr}_2\text{CaCu}_2\text{O}_8$ ($T_c = 90$ K) and of (ii) $\text{Bi}_{1.9}\text{Pb}_{0.1}\text{Sr}_2\text{CaCu}_2\text{O}_8$ ($T_c = 76$ K) postannealed in oxygen at 160 bars and 450°C . The experiments were performed using standard technique [6]. The symmetry labels used are the same as in the textbook by Tinkham [8] and refer to the tetragonal D_{4h} point group. Here, the pure B_{1g} and B_{2g} symmetries can be observed separately using crossed incident and scattering polarizations. For B_{2g} the polarization vectors are oriented parallel to the Cu-O bonds in the planes, for B_{1g} they are rotated by 45° .

Our theoretical considerations start from the expression for the general response function

$$\chi_{r,\gamma}(\mathbf{q}, \omega) = -T \sum_{i\omega_n} \sum_{\mathbf{k}} \text{Tr} \left[\hat{\Gamma}(\mathbf{k}, \mathbf{q}) \hat{G} \left(\mathbf{k} + \frac{\mathbf{q}}{2}, i\omega_n \right) \hat{\gamma}(\mathbf{k}, -\mathbf{q}) \times \hat{G} \left(\mathbf{k} - \frac{\mathbf{q}}{2}, i\omega_n - i\omega \right) \right], \quad (1)$$

in which $\hat{G}(\mathbf{k}, i\omega_n)$ denotes the Green's function in particle-hole or Nambu space [9] taken at the Matsubara frequency ω_n . The Nambu matrices $\hat{\gamma}$ and $\hat{\Gamma}$ denote the bare and renormalized vertices, respectively, which in turn determine the correlation function of interest, and Tr denotes taking the trace. We focus on the Raman vertex which describes the anisotropic mass fluctuations, $\hat{\gamma}(\mathbf{k}, \mathbf{q}) = \gamma(\mathbf{k}) \hat{\tau}_3$ with the Pauli matrix $\hat{\tau}_3$, for which Eq. (1) becomes identical to an expression derived by Klein and Dierker [3]. The limit of small \mathbf{q} can be taken as a consequence of the large optical penetration depth in the cuprates. Other choices of the vertices will be discussed in more detail in a forthcoming publication. For the limit where the energy of the incident light is small on the scale of the band energy the Raman vertex of non-resonant scattering is [10]

$$\gamma(\mathbf{k}) = m \sum_{\alpha,\beta} e_{\alpha}^S e_{\beta}^I \frac{\partial^2 \epsilon(\mathbf{k})}{\hbar^2 \partial k_{\alpha} \partial k_{\beta}} e_{\beta}^I, \quad (2)$$

where m is the electron mass, and $\mathbf{e}^{I,S}$ denote the vectors

of the incident and scattered light polarizations, respectively, and $\epsilon(\mathbf{k})$ denotes the conduction band dispersion. Thus, a variation of the polarization orientations allows one directly to probe mass fluctuations on different parts of the Fermi surface and exploit its symmetry. The crystal symmetry can be taken into account by expanding the bare ($\hat{\gamma}$) and renormalized ($\hat{\Gamma}$) vertices in terms of a complete set of crystal harmonics defined on the Fermi surface. For crystals of tetragonal symmetry, the basis set runs over the irreducible representations of the D_{4h} point group, and in general, many representations L contribute to Eq. (2). However, we will only consider the isotropic $L=0$ component and the $L=2$ components, arguing that more anisotropic components will be less dominant than the ones we consider.

The full gauge invariant treatment of Eq. (1) has been carried out via both a diagrammatic and a kinetic equation approach, using a gap function

$$\Delta(\mathbf{k}, T) = \Delta_0(T) [\hat{k}_x^2 - \hat{k}_y^2] \quad (3)$$

with a temperature-dependent gap maximum $\Delta_0(T)$. At zero temperature, the weak coupling result for the gap maximum is $\Delta_0(0)/k_B T_c = [\Delta_0(0)/k_B T_c]_{\text{BCS}} \exp(16/15)/2 = 2.5626$.

The treatment of the vertex corrections $\hat{\Gamma}$ due to the pairing interaction involves a discussion of the dynamics or fluctuations of the energy gap. The phase fluctuations of the order parameter lead to the occurrence of the gapless (massless) Goldstone, gauge or Anderson-Bogoliubov mode, which has to be accounted for in any response theory for superconductors because it ensures gauge invariance or equivalently charge conservation. The amplitude fluctuations of the gap, on the other hand, lead to the occurrence of (massive or "optical") order parameter collective modes with a gap in the excitation spectrum. For the density ($L=0$) channel we find that $\chi(\mathbf{q}=0, \omega) = 0$, which is a restatement of particle number conservation and bears out the gauge invariant nature of the theory. For the $L=2$ channels, we find that the Goldstone mode appears in the A_{1g} channel in addition to three massive modes which appear in the B_{1g} and E_g channels. It can be shown, however, that the massive modes are damped and have residues which approach zero as the position of the pole moves to zero frequency. The massive modes therefore do not drastically affect the spectrum [11]. We also included the vertex corrections due to the long range Coulomb interaction in our calculations. As a first consequence, we were able to show that the gauge mode drops out of the Raman response, in the same way as it does for the transverse current [12], and is of relatively little importance in the screened limit $\mathbf{q} \rightarrow 0$. Therefore, to a good approximation, Eq. (1) with $\hat{\Gamma}$ replaced by $\hat{\gamma}$ describes the gauge invariant Raman response. A second consequence of the Coulomb interaction is the complete screening of the isotropic density vertex [10]. Thus the only contribution to Raman scattering comes from energy bands with nonparabolic dispersion, i.e., the $L=2$ and higher terms. Furthermore we see that

since the A_{1g} channel has an isotropic component the response in the A_{1g} channel will be partially screened [13]. All other $L=2$ channels, however, will be unaffected by screening. Thus, the response at zero temperature is, in this case, simply given by

$$\chi''_{\gamma,\gamma}(\mathbf{q} \rightarrow 0, \omega) = \frac{N_F}{\omega} \text{Re} \left\langle \frac{|\gamma(\hat{\mathbf{k}})|^2 |\Delta(\hat{\mathbf{k}})|^2}{\sqrt{\omega^2 - 4|\Delta(\hat{\mathbf{k}})|^2}} \right\rangle. \quad (4)$$

Here $\langle \dots \rangle$ denotes an average over the Fermi surface (assumed to be spherical), N_F is the density of states for both spin projections at the Fermi level, and Re denotes taking the real part. The Raman response for three different symmetries is plotted in Fig. 1. One immediately recognizes the extreme sensitivity of the spectrum to polarization orientations. The maximum signal is seen at $\omega = 2\Delta_0$ only for the B_{1g} orientation while it is located at lower frequencies of roughly $1.3\Delta_0$ and $0.6\Delta_0$ for the B_{2g} and A_{1g} symmetries, respectively [14]. This is a feature which is present in all high- T_c compounds that have been studied via Raman scattering [4-7,15] and strongly suggests that the gap has predominantly B_{1g} character since any other gap symmetry will prevent the B_{1g} peak from being at the highest frequency.

Further, the spectrum rises slower in the B_{1g} channel compared to the other channels. The channel dependent asymptotic low frequency behavior is found as

$$\begin{aligned} \chi''_{\gamma,\gamma}(\omega \rightarrow 0) &\sim (\hbar\omega/2\Delta_0)^3 \ln|4\Delta_0/\hbar\omega|, \quad B_{1g} \\ &\sim \hbar\omega/2\Delta_0 \ln|4\Delta_0/\hbar\omega|, \quad A_{1g} \\ &\sim \hbar\omega/2\Delta_0, \quad B_{2g} \text{ and } E_g. \end{aligned} \quad (5)$$

The low temperature electronic Raman spectra of all cuprates show the same qualitative features [4-7,15]. For a quantitative comparison of theory and experiment, however, the Bi2:2:1:2 system is selected, because in this material class an almost perfect surface can be obtained, which allows us to use the raw data. Fits to the data on YBa₂Cu₃O₇ materials can be made using the theory although there are fundamental limitations connected with the chemistry and the structure of this specific compound. In Figs. 2 and 3 we show both experimental and theoretical results for the low energy part of the spectra in an as

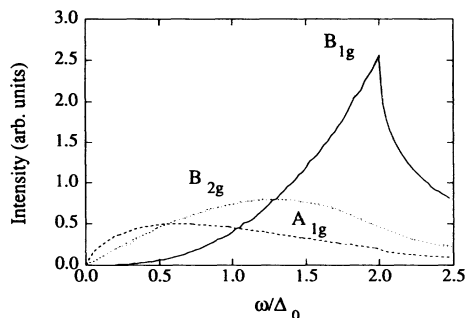


FIG. 1. Theoretical prediction of Raman spectra for B_{1g} , B_{2g} , and A_{1g} polarization orientations. The coefficients of the expansion of γ with respect to the $L=2$ crystal harmonics are all set equal to unity. The E_g spectra look identical to the B_{2g} spectra.

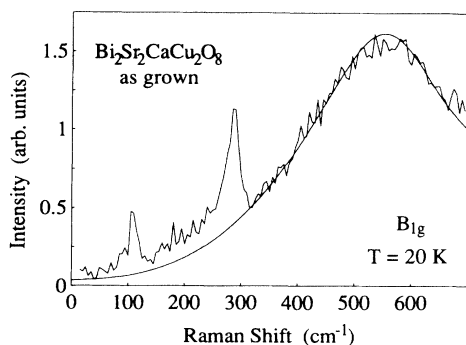


FIG. 2. The Raman spectrum in the B_{1g} channel as derived from Eq. (4) compared with experimental points. A value $2\Delta_0 = 574 \text{ cm}^{-1}$ has been used.

grown single crystal. We note that predictions concerning the overall magnitude of the spectra cannot be made without detailed band structure which determines the magnitude of the Raman vertices. This information is not presently available even for a simple metal such as aluminum [13]. The parameters used to obtain the best fit to the B_{1g} spectrum (Fig. 2) are $\Delta_0 = 287 \text{ cm}^{-1}$, a smearing width of $\Gamma/\Delta_0 = 0.15$ and $T = 20 \text{ K}$. The identical set of parameters is used for the B_{2g} spectra (Fig. 3). The quantity Γ/Δ_0 characterizes a convolution of the result (4) with a Gaussian distribution of maximum gaps Δ_0 to account for the experimental resolution and possible additional relaxation processes. For our model using $d_{x^2-y^2}$ pairing symmetry the peak position and the low frequency slopes [Eq. (5)] are immediately obtained for all polarizations. In contrast, an earlier comparison with an s -wave model [5] required a variation of the average gap energies of almost a factor of 2 and symmetry-dependent values of Γ/Δ_0 in the range from 0.28–0.7. In an independent lab, we have measured freshly cleaved samples of Bi2:2:1:2 grown elsewhere and the results are in excellent agreement with those of Figs. 2 and 3. We have also investigated an oxygen annealed sample, for which the spectral shape in the frequency regime $\omega < 2\Delta_0$ is similarly well reproduced. A discrepancy of roughly 10% in the position of the B_{2g} peak frequency may originate from additional imperfections introduced by the excess oxygen. In any case, our model fails to describe the spectra at high frequencies, $\omega \gg 2\Delta_0$, because the flat electronic continuum and polarization behavior of the frequency and temperature dependences cannot be reproduced without taking into account impurities and inelastic scattering [16]. A full description including both the normal and the superconducting state must unify both of these features and is beyond the scope of our paper.

Important information can also be obtained from the temperature dependence of the response in the limit of zero frequency shifts, i.e., the static response, particularly because vertex corrections vanish in this case and the influence of collisions is only relevant for nearly resonant impurity scatterers [17]. In this limit the ratio of the response in a superconductor to that of a normal metal is

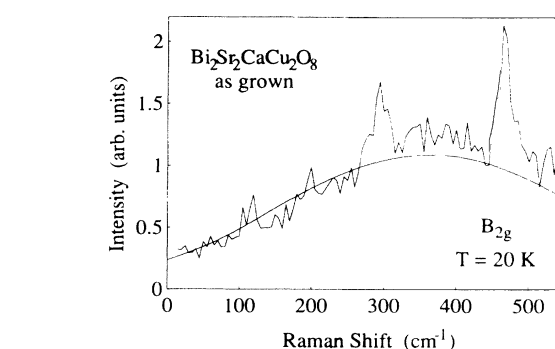


FIG. 3. The Raman spectrum in the B_{2g} channel as derived from Eq. (4) compared with experimental points. A value $2\Delta_0 = 574 \text{ cm}^{-1}$ has been used.

given by the compact expression

$$\frac{\chi''_S(\omega \rightarrow 0, T)}{\chi''_N(\omega \rightarrow 0, T)} = \frac{2\langle f(|\Delta(\hat{\mathbf{k}})|) |\delta\gamma(\hat{\mathbf{k}})|^2 \rangle}{\langle |\delta\gamma(\hat{\mathbf{k}})|^2 \rangle}, \quad (6)$$

where f is the Fermi function. Here $\delta\gamma(\hat{\mathbf{k}}) = \gamma(\hat{\mathbf{k}}) - \gamma_{L=0}$ due to the Coulomb screening. It is important to realize that the result (6) predicts a polarization dependence of the normalized Raman intensity at zero frequency, whenever the gap is anisotropic over the Fermi surface. In the case of an isotropic gap, the angular average over the vertices cancels out, leaving a polarization-independent ratio [17]. It turns out that Eq. (6) gives rise to an asymptotic low temperature behavior equivalent to the asymptotic low frequency behavior stated in Eq. (5), in the sense that ω may be replaced by T . This is shown in Fig. 4, where we plot our theoretical prediction for the normalized Raman intensity as a function of temperature. Note that, for certain symmetries, this temperature dependence is much weaker than in the isotropic BCS case, shown for comparison as the lowest curve. For the A_{1g} response, the intensity is 30% of the normal state value even at a temperature as low as $0.2T_c$, while for the B_{1g} case, the ratio is much smaller. This behavior has been seen in all cuprate systems investigated, where the small frequency residual scattering at approximately 20 K is smallest at the B_{1g} symmetry and substantially larger at polarizations projecting out the other symmetries [6] (compare

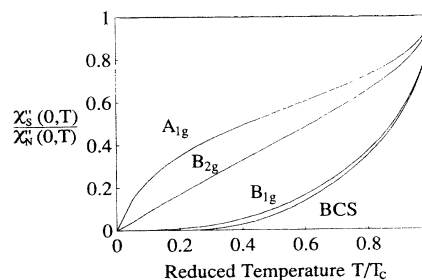


FIG. 4. Temperature dependence of the ratio of the Raman spectrum in the superconducting state to its normal state value in the limit of small frequency shifts, as derived from Eq. (6). The weak coupling temperature dependence of the gap has been used with $2\Delta_0(0)/k_B T_c = 5.1252$.

also Figs. 2 and 3). A quantitative experimental analysis of the temperature dependence of the gap using Eq. (6) would require the knowledge of the temperature dependence of $\chi_N''(\omega, T)$ for $T < T_c$. For superconductors with large H_{c2} , however, this information cannot be extracted from experiment and one might try to extrapolate the temperature dependence of the normal state response function to temperatures below T_c . Such a procedure is not unambiguous and we therefore leave a comparison of the residual scattering intensities with theory as a function of temperature below T_c for a forthcoming publication.

In conclusion we have seen that measurements of the electronic Raman effect on the cuprate systems provide a large body of symmetry dependent information all of which agree with the predictions of $d_{x^2-y^2}$ pairing. Of course at present the information from the Raman effect alone cannot completely rule out the notion of the existence of a finite minimum gap over the entire Fermi surface (e.g., the " $s+id$ " state investigated first by Kotliar [18] or the anisotropic s -wave gap discussed by Chakravarty *et al.* [19]) nor can it determine whether the gap changes sign around the Fermi surface. However, the theoretical analysis shows that the gap must be predominantly of B_{1g} character, and the low temperature and low frequency data seem to indicate that the minimum gap must be very small if it exists at all.

We are indebted to K. Andres, M. Cardona, B. S. Chandrasekhar, P. Fulde, R. Nematicschek, and C. Kendziora for many valuable discussions and suggestions. One of the authors (T.P.D.) would like to thank the Max-Planck-Institut für Festkörperforschung in Stuttgart for financial support and another (D.H.L.) would like to thank the Alexander von Humboldt Foundation. This work has partly been supported by the Bayerische Forschungsförderung via the Forschungsverbund Hochtemperatursupraleiter (FORSUPRA).

*Present address: Department of Physics, University of California, Davis, CA 95616.

†Present address: Physics Division, P-10, Los Alamos, NM 87545.

- [1] D. J. Scalapino, E. Loh, and J. E. Hirsch, *Phys. Rev. B* **34**, 8190 (1986); P. Monthoux, A. V. Balatsky, and D. Pines, *Phys. Rev. Lett.* **67**, 3449 (1991), and references therein; D. J. Scalapino (to be published).
- [2] P. C. Hammel, M. Takigawa, R. H. Heffner, Z. Fisk, and K. C. Ott, *Phys. Rev. Lett.* **63**, 1992 (1989); W. N. Hardy, D. A. Bonn, D. C. Morgan, R. Liang, and K. Zhang, *Phys. Rev. Lett.* **70**, 3999 (1993).
- [3] M. V. Klein and S. B. Dierker, *Phys. Rev. B* **29**, 4976 (1984); H. Monien and A. Zawadowski, *Phys. Rev. B* **41**, 8798 (1990).
- [4] S. L. Cooper, M. V. Klein, B. G. Pazol, J. P. Rice, and D. M. Ginsberg, *Phys. Rev. B* **37**, 5920 (1988); R. Hackl, in *Electronic Properties of High- T_c Superconductors and Related Compounds*, edited by H. Kuzmany, M. Mehring, and J. Fink, Springer Series in Solid-State Sciences Vol. 99 (Springer, Berlin, 1991).
- [5] R. Hackl, W. Gläser, P. Müller, D. Einzel and K. Andres, *Phys. Rev. B* **38**, 7133 (1988); S. L. Cooper, F. Slakey, M. V. Klein, J. P. Rice, E. D. Bukowski, and D. M. Ginsberg, *Phys. Rev. B* **38**, 11934 (1988).
- [6] T. Staufer, R. Nematicschek, R. Hackl, P. Müller, and H. Veith, *Phys. Rev. Lett.* **68**, 1069 (1992).
- [7] R. Nematicschek, T. Staufer, O. V. Misochko, D. Einzel, R. Hackl, P. Müller, and K. Andres, in *Electronic Properties of High- T_c Superconductors and Related Compounds* (Ref. [4]).
- [8] M. Tinkham, *Group Theory and Quantum Mechanics* (McGraw-Hill, New York, 1964).
- [9] Y. Nambu, *Phys. Rev.* **117**, 648 (1960).
- [10] A. Abrikosov and V. M. Genkin, *Zh. Eksp. Teor. Fiz.* **65**, 842 (1973) [*Sov. Phys. JETP* **38**, 417 (1974)].
- [11] It can be shown that the response in the B_{1g} channel is the least affected by the vertex corrections, while the peak position in the other channels can be slightly modified.
- [12] P. J. Hirschfeld and D. Einzel, *Phys. Rev. B* **47**, 8837 (1993).
- [13] We point out that the screening of the A_{1g} channel seems to indicate that the A_{1g} spectrum should be smaller than the spectra in the other channels (see Fig. 1), although what has usually been labeled the " A_{1g} " channel ($\mathbf{x}\mathbf{x}$ or $\mathbf{x}'\mathbf{x}'$ configurations) experimentally displays a large signal. However, this is misleading due to several factors. First, it is important to note that in contrast to all other channels the A_{1g} channel cannot be individually accessed by in-plane scattering geometries and one always measures a combination of A_{1g} and either $B_{1g}(\mathbf{x}\mathbf{x})$ or $B_{2g}(\mathbf{x}'\mathbf{x}')$ components with prefactors ≥ 1 . Second, the overall magnitude of the spectrum is governed by the magnitude of the Raman vertices γ , which are in principle derivable from real band structure but are presently only known for a very small number of materials. We note that the A_{1g} vertex, however, will in most cases be quite large since it selects the most isotropic components of the full Raman tensor for the $L=2$ subgroup. An estimate derivable from simple band structure would suggest that $\gamma_{A_{1g}} \sim \gamma_{B_{1g}} \sim t$, while $\gamma_{B_{2g}} \sim t'$, with t, t' the nearest- and next-nearest-neighbor hopping parameters, respectively, leading to the conclusion that the magnitude of the spectra in the B_{2g} channel should be smaller than the other channels by a factor of $(t/t')^2$. Thus it is quite plausible that both the $\mathbf{x}\mathbf{x}$ and $\mathbf{x}'\mathbf{x}'$ spectra can be quite large.
- [14] This indicates that the energy gap can only be identified with the peak position in the B_{1g} channel, and the temperature dependence of the peak position will most closely follow its true form only in this channel. However, it is to be noted that impurities will also change the position of the peak away from $2\Delta_0$ even in this channel (see Ref. [17]), making the identification of the gap from the peak maximum less precise.
- [15] R. Nematicschek, O. V. Misochko, B. Stadlober, and R. Hackl, *Phys. Rev. B* **47**, 3450 (1993).
- [16] A. Virostek (private communication); A. Zawadowski and M. Cardona, *Phys. Rev. B* **42**, 10732 (1990).
- [17] T. P. Devereaux, *Phys. Rev. B* **45**, 12965 (1992); **47**, 5230 (1993).
- [18] G. Kotliar, *Phys. Rev. B* **37**, 3664 (1988).
- [19] S. Chakravarty, A. Sudbø, P. W. Anderson, and S. Strong, *Science* **261**, 337 (1993).